



Morphology of cellulose objects regenerated from cellulose-N-methylmorpholine N-oxide-water solutions

Olga Biganska, Patrick Navard

► To cite this version:

Olga Biganska, Patrick Navard. Morphology of cellulose objects regenerated from cellulose-N-methylmorpholine N-oxide-water solutions. Cellulose, Springer Verlag, 2009, 16 (2), pp.Pages 179-188. <10.1007/s10570-008-9256-y>. <hal-00508367>

HAL Id: hal-00508367

<https://hal-mines-paristech.archives-ouvertes.fr/hal-00508367>

Submitted on 10 Dec 2012

HAL is a multi-disciplinary open access archive for the deposit and dissemination of scientific research documents, whether they are published or not. The documents may come from teaching and research institutions in France or abroad, or from public or private research centers.

L'archive ouverte pluridisciplinaire **HAL**, est destinée au dépôt et à la diffusion de documents scientifiques de niveau recherche, publiés ou non, émanant des établissements d'enseignement et de recherche français ou étrangers, des laboratoires publics ou privés.

Morphology of cellulose objects regenerated from cellulose- *N*-methyilmorpholine *N*-oxide-water solutions

Olga Biganska* and Patrick Navard**

Mines ParisTech, CEMEF- Centre de Mise en Forme des Matériaux, CNRS UMR
7635, BP 207 1 rue Claude Daunesse 06904 Sophia Antipolis Cedex, France.

Member of the European Polysaccharide Network of Excellence (EPNOE),
www.epnoe.eu

* Present address: L'Oréal, 188-200, rue Paul Hochart 94550 Chevilly-Larue,
France

** To whom correspondence should be addressed

Tel.: +33 (0)4 93 95 74 66; fax: +33 (0)4 92 38 97 52

e-mail: patrick.navard@mines-paristech.fr

ABSTRACT

The precipitation in aqueous media of cellulose from solutions in *N*-methylmorpholine *N*-oxide (NMMO) hydrates is an important stage in the process of manufacturing of fibres, films and other cellulose objects. It is responsible for the formation of the structure of the regenerated object and their morphological characteristics significantly influence the properties of the final products. Regeneration of rather large cellulose objects was observed in situ by optical microscopy. It was found that all regenerated objects present an asymmetric structure composed of a dense skin surrounding a sub-layer characterised by the presence of finger-like voids. The porous texture of the cellulose parts between these voids is typical of the one obtained by spinodal decomposition. The morphologies of regenerated cellulose samples are described as a function of various parameters, initial cellulose solutions and composition and temperature of the aqueous regeneration bath. A mechanism of the structure formation during regeneration is proposed.

KEY-WORDS

Cellulose, *N*-methylmorpholine *N*-oxide, Lyocell, regeneration, morphology

INTRODUCTION

N-methylmorpholine-*N*-oxide (NMMO) hydrates are direct solvents for cellulose, used commercially in the preparation of homogenous cellulose-NMMO-water solutions (dope) for making mainly fibres (Lyocell process). The production of the cellulose objects by the NMMO process passes through the step of regeneration of the spun or extruded dope in a coagulation bath (Krüger 1994). In order to regenerate cellulose-NMMO-water solution, the liquid coagulating agent must be a solvent for NMMO and a non-solvent for cellulose. Polar liquids, like water or alcohol, are used as coagulation bath because they are miscible with NMMO and cause NMMO removal from the cellulose solution. It is expected that the regeneration of cellulose-NMMO-water solutions follows the well known principles of phase separation in polymer solutions valid in membrane formation, Koenhen et al (1977), Broens et al (1980), Shen and Cabasso (1982), Radovanovic et al (1992), Pereira Nunes and Inoue (1996), Tsay and McHugh(1992), Barton et al (1997).

When a polymer solution is regenerated in a non-solvent coagulation bath, the resultant objects have an asymmetric structure, i.e. a more or less dense skin is supported by a porous sub-layer. The formation of the skin results from the increase in polymer concentration stimulated by an extremely rapid solvent depletion from the top layer of the solution. Two predominant morphologies – finger-like and sponge-like – are usually observed in the sublayer (Broens et al 1980, Shen and Cabasso 1982). The way these morphologies are forming depends on the rate of precipitation of the polymer that is determined by the rate of solvent diffusing out of, and the rate of non-solvent diffusing into, the polymer solution at the interface. Finger-like morphologies are formed when the non-solvent enters into a polymer

solution faster than the solvent diffuses out. Sponge-like structures are formed when the solvent diffuses out faster than the non-solvent diffuses in (Shen and Cabasso 1982, Barton et al 1997).

The relations between the mechanisms of phase separation and the process of structure formation are still a matter of active research, owing to their importance in the processing of polymer membranes. Changes in composition bring a ternary polymer/solvent/non-solvent system to a condition which favours liquid-liquid or solid-liquid phase separation. Solid-liquid phase separation is considered in structure formation of systems containing crystallisable polymers. Liquid-liquid phase separation is considered for systems containing either amorphous or crystallisable polymers. In the case of liquid-liquid demixing of polymer solutions, two different mechanisms can happen: nucleation and growth or spinodal decomposition. Most of the earlier papers ascribe the formation of the structure in membranes produced by regeneration of a polymer solution in a non-solvent coagulation bath to the nucleation and growth mechanism. The importance of spinodal decomposition, that is very rapid and difficult to quantify, has been recognised more recently (Radovanovic et al 1992, Pereira Nunes and Inoue 1996).

As far as the regeneration of cellulose-NMMO-water solutions is concerned, several publications describing the morphological features of fibres and films are available (Romanov et al 1988, Bang et al 1999, Fink et al 2001, Laity et al 2002). Romanov et al. (1988) noted that the regeneration of fibres in a bath of isopropyl alcohol increases their microporosity ($0.1\mu\text{m}$) and creates vacuoles in the structure in comparison with a water bath. Fink et al. (2001) reported that fibres precipitated in water show a dense cellulose network structure with small finely distributed voids with dimensions ranging from 10 to 100nm. This structure seems to be uniform

throughout the cross-section, except for a small boundary layer with highly densified material. The authors also investigated the regeneration in various alcohols and observed that the increase of their molecular mass leads to the formation of a distinct skin-core structure. Laity et al. (2002) studied the composition and phase changes during the regeneration of cellulose-NMMO-water solutions in water. They reported that the cross section of regenerated solution observed by SEM appeared uniformly dense. TEM observation revealed porosity on the scale of a few nanometres.

Crawshaw and Cameron (2000) show that there is a network of voids elongated in the fibre direction. In the untreated wet state, there are many small voids (mean length 36 nm, mean thickness 0.3 nm) while in the dry state after drying at 160°C, there is a much lower overall volume fraction of much larger pores voids (mean length 270 nm, mean thickness 5 nm). Jianchin et al. (1999) have reported the presence of a skin-core structure in Lyocell fibres. Swelling experiments performed in aqueous NaOH solutions and swollen fibres investigation with an environmental scanning electron microscope allowed the authors to suggest that Lyocell fibres are made of a composite skin and of a crystalline core formed by parallel fibrils. The skin is amorphous and very elastic. Its thickness is estimated to be between 57 and 177 nm (average value is equal to 73 nm). The skin is made up of two layers: the outer layer is very thin while the inner one is thicker. Cellulose chains in the outer layer are less oriented than chains in the inner layer. The core of the fibre is made up of highly oriented parallel fibrils and amorphous regions connecting these fibrils. Some pores and defects could be also present in the amorphous regions.

Abu-Rous et al. (2006) showed that Lyocell fibres contain only nanopores in the core of the fibre and a very porous skin layer. Schurz et al. (1995) proposed a structural model for fibres spun from cellulose-NMMO-water solutions. The

orientation of both crystalline and amorphous zones was reported to be very high. Crystalline regions have rather isolated fibrils that can be easily separated by a mechanical treatment, leading to fibrillation (Ducos et al 2006). A recent work Abu-Rous et al. (2007) based on dye penetration proposes to distinguish three regions inside Lyocell fibres, a skin layer with a compact structure, a porous middle zone and a compact fibre centre.

The understanding of the structure formation during coagulation and the morphology of regenerated cellulose-NMMO-water solutions, depending on the regeneration kinetics, is essential for the properties of cellulose objects produced by NMMO process. The main objective of this work is the investigation of the morphologies of regenerated cellulose-NMMO-water solutions as a function of various parameters of both cellulose solutions and coagulation baths. These observations will be linked to the knowledge of the regeneration kinetic parameter obtained before (Biganska and Navard 2005).

EXPERIMENTAL PART

Cellulose-NMMO-water solutions were prepared in the R&D department of the Austrian company Lenzing AG using the method described previously (Biganska and Navard 2005). Several cellulose pulp samples and different cellulose concentrations were used in this study in order to describe the influence of these parameters on the morphology of regenerated solutions. Four different pulp families called Krafts 1-4 were used in this work. Each Kraft family has the same cellulose origin, the difference being the molecular weight distribution (Table 1). The

Location of
table 1

properties of the cellulose samples as well those of the cellulose solutions were described elsewhere (Biganska and Navard 2005).

NMMO-water mixtures with initial NMMO concentration varying from 0% (pure water) to 50% were used for coagulation baths. The required mixtures were prepared by the dilution of the solution containing 50% of NMMO provided by Aldrich.

The regeneration of the cellulose solutions was performed with two types of cellulose solution physical states. First, with solid (crystallised) cellulose-NMMO-water solutions shaped by a press to obtain discs of definite thickness (1mm and 3mm) and diameter (20mm). Second, with molten, 2 to 3mm thick cellulose-NMMO-water solutions. Samples were molten at 90°C.

Each cellulose solution sample was immersed into a coagulation bath to regenerate it, i.e. to transform the polymer solution into a pure, highly swollen cellulose object. Then, the regenerated cellulose sample was cut with a razor blade in order to obtain a thin slice. These slices were then observed with an optical microscope (Leitz Metallux 3) and an environmental scanning electron microscope (Philips XL ESEM). In order to observe the regenerated solutions in a wet state, the scanning electron microscope was equipped with a Peltier stage. This device allows keeping the sample in the electron microscope chamber in an atmosphere of a desired humidity ratio fixed by two parameters, the pressure and the temperature.

RESULTS AND DISCUSSION

Influence of the state of the cellulose solution before regeneration on the morphology of the regenerated objects

If before being immersed into the regenerating bath, the cellulose solution is solid (crystallized) or liquid (in a molten state), the morphologies of the regenerated cellulose objects are very different. In the case of a solid solution obtained by cooling the solution, it was shown (Biganska et al 2002) that it is the solvent which is crystallizing. This is leading a variety of morphologies like large spherulites. After sublimation of NMMO and water, cellulose chains retain the general morphology of the crystallised solution (Chanzy et al 1979). The same phenomenon is observed if such a crystallized solution is regenerated in an aqueous bath. Figure 1 illustrates this phenomenon for the regeneration of a 3wt% cellulose solution in a water bath. The right (regenerated) and left (solution) sides of the picture show that they have the same morphology. This is due to the fact that the solvent is crystallizing, pushing cellulose chains out of the crystals but keeping them very close to the tiny crystals, keeping thus the image of the crystal arrangements. When the crystals are dissolving in the regeneration liquid, cellulose chains keeps the same organisation they had around the solvent crystals. There is no phase separation involving cellulose during the regeneration of a solid crystallized cellulose solution since the phase separation between the solvent and cellulose had already occurred during the crystallisation of the solvent. The observation of the cross-section of the solutions regenerated in a water bath after crystallisation reveals a uniform and compact structure with few voids. As we will see, voids are originating from liquid-liquid phase separation, a case not occurring here.

Location of
fig 1

The situation is completely different after the regeneration of a molten solution. In this case the observation of the cross-section reveals a skin-core structure as illustrated in Figure 2.

Location of
fig 2

The thickness of the dense skin is not uniform along the perimeter of the sample. The core contains finger-like voids that can occupy either the whole surface of the cross-section or form a crown. The texture of the cellulose material that forms the walls of the finger-like cavities has micrometer-scale porosity. In the following we will describe in details the structure obtained after the regeneration of molten cellulose-NMMO-water solutions and the parameters that influence it.

Fingering in regenerated objects obtained from a molten solution

Formation of the finger-like patterns is a common feature in liquid-liquid demixing. The classic example is the Staffman-Taylor fingers (Saffman and Taylor 1958, Kessler et al 1988), observed when air drives water from a Hele-Shaw cell (two parallel plates with a narrow gap of constant thickness between them). A moving air-liquid interface is driven by the gradient of a diffusive field. Planar or circular interfaces are morphologically unstable and tend to finger, along directions favoured by the boundary conditions and/or anisotropy. The difference between the morphologies of the cellulose solutions regenerated in the molten or solid crystallised states are thus clear. Finger-like voids are formed when a low viscosity fluid is displacing a more viscous one. So, finger-like voids are formed in the molten solutions in contact with water of the coagulation bath (viscosity of water is much lower than the viscosity of any cellulose solution). In contrast, there is no moving liquid-liquid interface during the regeneration of a crystallised solution. The dissolution of the crystallised NMNO is only due to the fact that NMMO is highly hygroscopic (Navard and Haudin 1981). The few observed voids in the regenerated objects from solid crystallized solutions are due to defects like air bubbles.

On the basis of what is known from the theory of membranes formation and taking into account our own observations, the following mechanism of the formation of structure during the regeneration of molten cellulose-NMMO-water solutions can be proposed. The contact between the solution and the liquid from the coagulation bath leads to the rapid outflow of the solvent from the top layer of the solution. The polymer profile at the point of precipitation exhibits a very high interfacial concentration, thus favouring the formation of a dense skin immediately after immersion of the sample into the coagulation bath. The bulk of the sample is at near the initial concentration and is in a fluid state. Thus, a rapid inflow of the coagulant can take place through the weak spots at the skin interface. Rapid growth of finger-like voids in the fluid region under the skin occurs due to the moving interface created by the coagulant (less viscous) and the solution (more viscous). Measurements of the coefficients of diffusion of NMMO solvent from the solution into the bath and of the coagulant from the bath into the solution (Biganska and Navard 2005) show that the inflow of the coagulant is one order of magnitude higher than the outflow of the solvent. This result is in agreement with the fact that the formation of a finger-like structure is favoured when the non-solvent enters the sample more rapidly than the solvent exits from it (Shen and Cabasso 1982).

Influence of the concentration of cellulose, the nature and the temperature of coagulation bath on the morphology of regenerated solutions

Cellulose concentration

Location of
fig 3

Molten solutions with 3wt% of cellulose, 82wt% of NMMO and 15wt% of water were regenerated in a water bath at room temperature. The morphology was very similar, independent on the characteristics of the Kraft samples. The observation of

the cross-sections reveals the presence of a skin surrounding finger-like voids. The thickness of the skin is about 100 μm . A regular ordering of voids is seen near the skin and a more disordered distribution is found in the centre of the samples. The length of voids can reach 500 μm and the width 50 μm . To illustrate this, Figure 3 presents a scanning electron microscopy image of the cross-section of the regenerated solution prepared with the Kraft 3 pulp. Molten solutions with 6wt%, 8wt% and 10wt% of cellulose were regenerated in water bath at room temperature in order to test the influence of cellulose concentration on the morphology of regenerated solutions. Figure 4 shows the scanning electron micrographs, taken at various magnifications, of the cross-section of the 6wt% cellulose solution regenerated in a water bath. Figure 4a shows a general view of the cross-section where one can distinguish the skin and the voids. Figure 4b, taken in a place close to the sample centre, shows some smaller voids. Figures 4c and 4d are showing the aspect of the walls between voids. The analysis of numerous samples reveals that the ordering of voids observed for the samples with low cellulose concentration decreases when the cellulose concentration increases. The length of voids decreases while their width increases when the concentration of cellulose increases. Both effect are most probably due to the viscosity of the highly concentrated, cooled solution. The difficulty to displace large amounts of cellulose chains restricts the propagation of the fingering instability, and disrupts its regular formation. In fact, the lengths of the voids observed in the 6wt% cellulose samples are ranging between 400 and 500 μm and their width is of about 30 μm . The corresponding dimensions are of 300 μm and 50 μm for the samples with 8wt% of cellulose. In the case of solutions with 10wt% of cellulose, these dimensions are of 200 μm and 50 μm . It seems that the thickness of the skin also increases with cellulose concentration.

Location of
fig 4

NMMO concentration in regenerated bath

The effect of the concentration of NMMO in the initial aqueous bath used for regeneration was tested on 6wt% cellulose solutions. The observation of the cross-sections of the samples regenerated in the baths with 0% (pure water), 10%, 20%, 30%, 40% and 50% of NMMO reveals that finger-like voids become less numerous when the concentration of NMMO increases (Fig 5). This is due to the fact that we have a very “strong” precipitation in pure water while the regeneration is “weak” in the presence of NMMO. The higher the NMMO concentration in the regenerating bath is, the less rapidly this fluid is penetrating in the cellulose solution. The fingering mechanism is thus less favoured.

Location of
fig 5

Regenerating bath temperature

The effect of the temperature of water bath on the morphology of regenerated solutions can be illustrated on the example of 8wt% cellulose solutions. Figure 6 gives the scanning electron micrographs of the cross-sections of the solutions regenerated at 20°C, 50°C and 80°C. The left column shows the evolution of general morphology while the right column presents the evolution of the material texture between the voids. It can be seen that the thickness of the skin decreases, the number of voids increases and their width decreases when the bath temperature increases. Another effect of the temperature increase is the appearance of a dense part in the middle of the samples and, consequently, the confinement of the void region in a corona.

Location of
fig 6

Mechanisms of cellulose-regenerating medium phase separation

Location of
fig 7

The cross-sections of molten solutions with 8wt% (a) and 12wt% cellulose (b) regenerated in water bath at 50°C have a microporous globular texture (Fig 7) made by the juxtaposition of small spheres of 1-2 μ m (Fig 6a). Such a texture is present in almost all the investigated samples obtained from a molten initial state. This texture is due to the phase separation mechanism. Two mechanisms of phase separation can take place during liquid-liquid demixing of polymer solutions, either nucleation and growth where the nuclei of one phase grow in the mixture or spinodal decomposition where a periodic variation of concentration leads to the final phase separation. If there is a clear difference between these two mechanisms in their first stages (nucleation and growth shows isolated entities while spinodal decomposition has a 3D network-like morphology), both tends to the same spherical morphology at the end, due to surface tension effects. If there is no external nucleation agent in the mixture, nucleation and growth gives a morphology composed of spheres of different diameters (due to the sporadic nucleation), positioned randomly in the regenerated material while spinodal decomposition gives rather monodisperse spheres, usually ordered along lines (this is due to the 3D-network like structure of the cellulose-rich phase). The micrographs shown on Figure 6 clearly suggest that the phase separation mechanism is spinodal decomposition in the case of the regeneration of a molten cellulose-NMMO solution in a water bath. Picture 6b, seldom observed, represents a frozen periodic structure while the picture 6a, frequently seen, corresponds to the periodic structure after it breaks down. This conclusion is supported by independent observations made on cellulose objects regenerated from NMMO solutions (Zhang and Shao 2001), (Mortimer and Peguy 1996) or during regeneration by NMR (Laity et al. 2002).

CONCLUSION

The type of morphology of a regenerated cellulose object from a cellulose solution in *N*-methylmorpholine *N*-oxide-water is not very much dependent on the cellulose concentration or the bath composition. It is strongly dependent on the state of the solution prior to regeneration. If the solution has crystallised, a dense morphology is observed while a dense skin surrounding a core made of large voids with cellulose walls is obtained from a molten solution. In this latter case, the cellulose wall structure (small ordered spherical objects) is due to a spinodal decomposition.

Further investigations on the details of the fast spinodal decomposition by light scattering and on the formation of the very thin skin during regeneration would help the understanding of the morphology development of objects regenerated from NMMO-cellulose solutions.

REFERENCES

Abu-Rous M, Ingolic E, Schuster KC (2006) Visualisation of the fibrillar and pore morphology of cellulosic fibres applying transmission electron microscopy, *Cellulose* 13:411-419

Abu-Rous M, Varga K, Bechtold T, Schuster KC (2007) A new method to visualize and characterize the pore structure of Tencel (Lyocell) and other man-made cellulosic fibres using a fluorescent dye molecular probe, *J Appl Polym Sci* 106: 2083-2091

Bang YH, Lee S, Park JB, Cho HH (1999) Effect of coagulation conditions on fine structure of regenerated cellulosic films made from cellulose/*N*-methylmorpholine-*N*-oxide/H₂O systems. *J Appl Polym Sci* 73: 2681-2690

Barton BF, Reeve JL, McHugh AJ (1997) Observations on the dynamics of nonsolvent-induced phase inversion. *J Polym Sci Part B: Polym Phys* 35:569-585

Biganska O, Navard P, Bedue O (2002) Crystallisation of cellulose/*N*-methylmorpholine *N*-oxyde hydrates solutions. *Polymer* 43:6139-6145

Biganska O, Navard P (2005) Kinetics of precipitation of cellulose from cellulose-NMMO-water solutions. *Biomacromolecules* 6:1949-1953

Broens L, Altena FW, Smolders CA, Koenhen DM (1980) Asymmetric membrane structures as a result of phase separation phenomena. *Desalination* 32:33-45

Chanzy H, Dubé M, Marchessault RH (1979) Crystallization of cellulose with N-methylmorpholine N-oxide: A new method of texturing cellulose. *J Polymer Sci Polym Lett Ed* 17:219-226

Crawshaw J, Cameron RE (2000) A small angle X-ray scattering study of pore structure in Tencel[®] cellulose fibres and the effects of physical treatments. *Polymer*, 41:4698

Ducos F, Biganska O, Schuster KC, Navard P (2006) Influence of the Lyocell fibre structure on their fibrillation. *Cell. Chem. Techn.* 40(5):299-311

Fink H-P, Weigel P, Purz HJ, Ganster J (2001) Structure formation of regenerated cellulose materials from NMMO-solutions. *Progr Polym Sci* 26:1473-1524)

Jianchin Z, Meiwu S, Zhu H, Kan L (1999) Study of the skin-core structure of lyocell staple fibers. *Chemical Fibers International*, 49:496-500

Kessler DA, Koplik J, Levine H (1988) Pattern selection in fingered growth phenomena. *Adv Phys* 37:255-339

Koenhen DM, Mulder MHV, Smolders CA (1977) Phase separation phenomena during the formation of asymmetric membranes. *J Appl Polym Sci* 21:199-215

Krüger R (1994) Cellulosic filament yarn from the NMMO Process. Lenzinger Berichte 9:49-52

Laity PR, Glover PM, Hay JN (2002) Composition and phase changes observed by magnetic resonance imaging during non-solvent induced coagulation of cellulose. Polymer 43:5827-5837

Mortimer SA, Péguy A (1996) Methods for reducing the tendency of lyocell fibers to fibrillate, Journal of Applied Polymer Science. 60:305-316

Navard P, Haudin JM (1981) Etude thermique de la *N*-méthylmorpholine *N*-oxyde et de sa complexation avec l'eau. J Thermal Anal 22:107-118

Pereira Nunes S, Inoue T (1996) Evidence for spinodal decomposition and nucleation and growth mechanisms during membrane formation. J Membrane Sci 111:93-103)

Radovanovic P, Thiel SW, Hwang S-T (1992) Formation of asymmetric polysulfone membranes by immersion precipitation. Part II. The effects of casting solution and gelation bath compositions on membrane structure and skin formation. J Membrane Sci 65:231-246

Romanov VV, Sokira AN, Lunina OB, Iovleva MM (1988) Morphological features of the structure of fibres prepared from solutions of cellulose in methylmorpholine oxide *Fibre Chemistry* 20:38-39; *Khimicheskie Volokna* 1:27–28

Saffman PG, Taylor GI (1958) The penetration of fluid into a porous medium or Hele-Shaw cell containing a more viscous liquid. *Proc Royal Soc London A* 245:312-329

Schurz J, Lenz J, Wrentschur E (1995) Inner surface and void system of regenerated cellulose fibers. *Die Angewandte Makromolekulare Chemie*, 229:175-184

Shen TC, Cabasso I (1982) *Macromolecular Solutions, solvent-property relationship in polymers*, R.B. Seymour and G.A. Stahl, Eds., Pergamon Press, New-York 108

Tsay CS, McHugh AJ (1992) A rationale for structure formation during phase inversion. *J Polym Sci: Part B: Polym Phys* 30:309-313

Zhang Y, Shao H, Wu C, Hu (2001) Formation and Characterization of Cellulose Membranes from N-Methylmorpholine-N-oxide Solution *Macromolecular Bioscience*. 1 :141-148

Captions for Tables and Figures.

Table 1 Characteristics of the cellulose used for the preparation of cellulose/NMMO/water solutions. Molar mass distribution was measured by size exclusion chromatography (SEC/GPC) and crystallinity by Fourier transform infrared spectrometry (FT-IR). From Biganska and Navard 2005.

Figure 1 Optical micrograph of the moving interface created during the regeneration of a solid cellulose-NMMO-water solution in a water bath.

Figure 2 Schematic representation of the cross-section of the regenerated cellulose samples : solution regenerated after crystallisation (left) and solution regenerated in molten state (right).

Figure 3 Scanning electron micrograph of the cross-section of a 3wt% cellulose solution regenerated in a water bath at room temperature.

Figure 4 Scanning electron micrographs of the cross-sections of a 6wt% cellulose solution regenerated in a water bath at room temperature : a) general view, b) voids, c) and d) aspect of walls between voids.

Figure 5 Scanning electron micrographs of the cross-sections of a molten 6wt% cellulose solution regenerated in a NMMO water bath at room temperature with varying NMMO content in the bath.

Figure 6 Scanning electron micrographs of the cross-sections of a 8wt% cellulose solution regenerated in a water bath at different temperatures.

Figure 7 Scanning electron micrographs of the fine structure observed in regenerated cellulose-NMMO-water solutions with initial concentration of cellulose of 8wt% (a) and 12wt% (b).

Table 1

| | Kraft 1/1 | Kraft 1/2 | Kraft 2/1 | Kraft 2/2 | Kraft 3 | Kraft 4 |
|------------------------------|------------------|------------------|------------------|------------------|----------------|----------------|
| Mn (x1000) | 77.4 | 44.2 | 53.0 | 40.4 | 50 | 51.7 |
| Mw (x1000) | 226.3 | 90.2 | 155.0 | 98.2 | 207 | 105.2 |
| Mz (x1000) | 468.9 | 158.0 | 410.5 | 206.9 | 619.9 | 186.7 |
| wt % (DP<50) | 1.1 | 1.6 | 1.5 | 2.3 | 2.6 | 1 |
| wt % (DP<200) | 7.8 | 18.5 | 14.3 | 21.8 | 15.8 | 14.6 |
| wt % (DP>2000) | 21 | 2 | 10.8 | 4 | 18 | 3.5 |
| Crystallinity [%] | 53 | 55 | 51 | 47 | 46 | 43 |

Figure 1

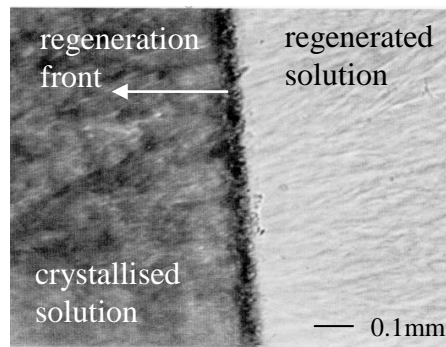


Figure 2

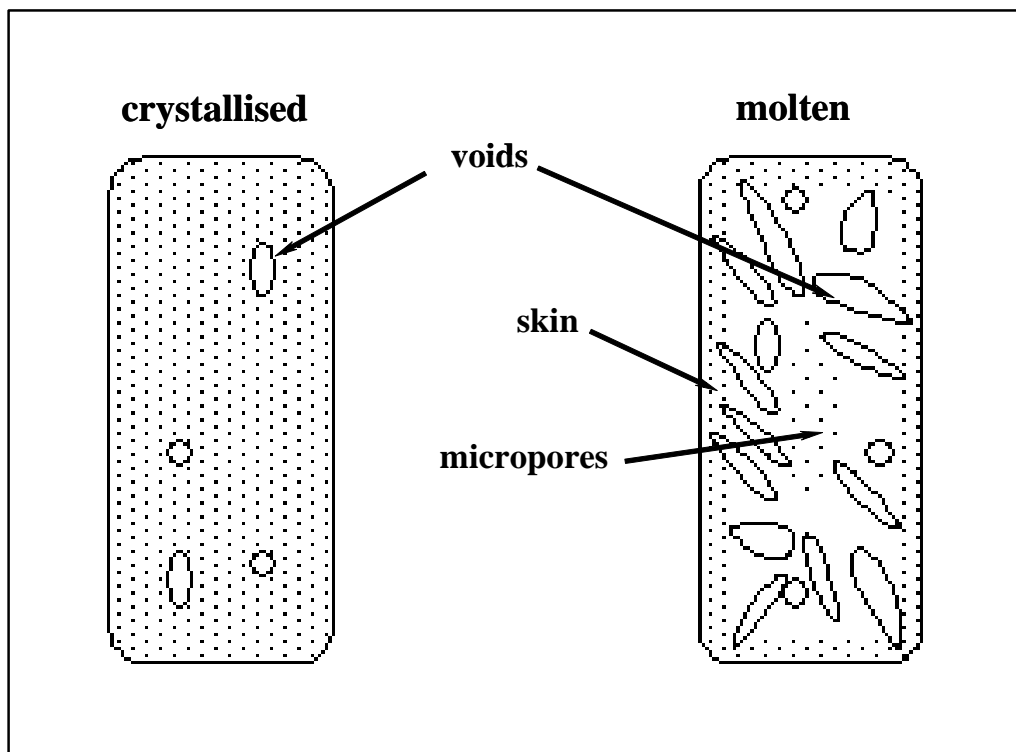


Figure 3

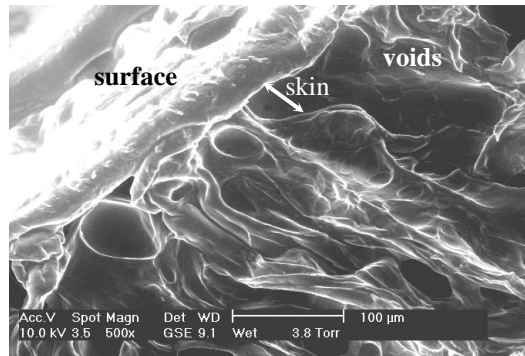


Figure 4

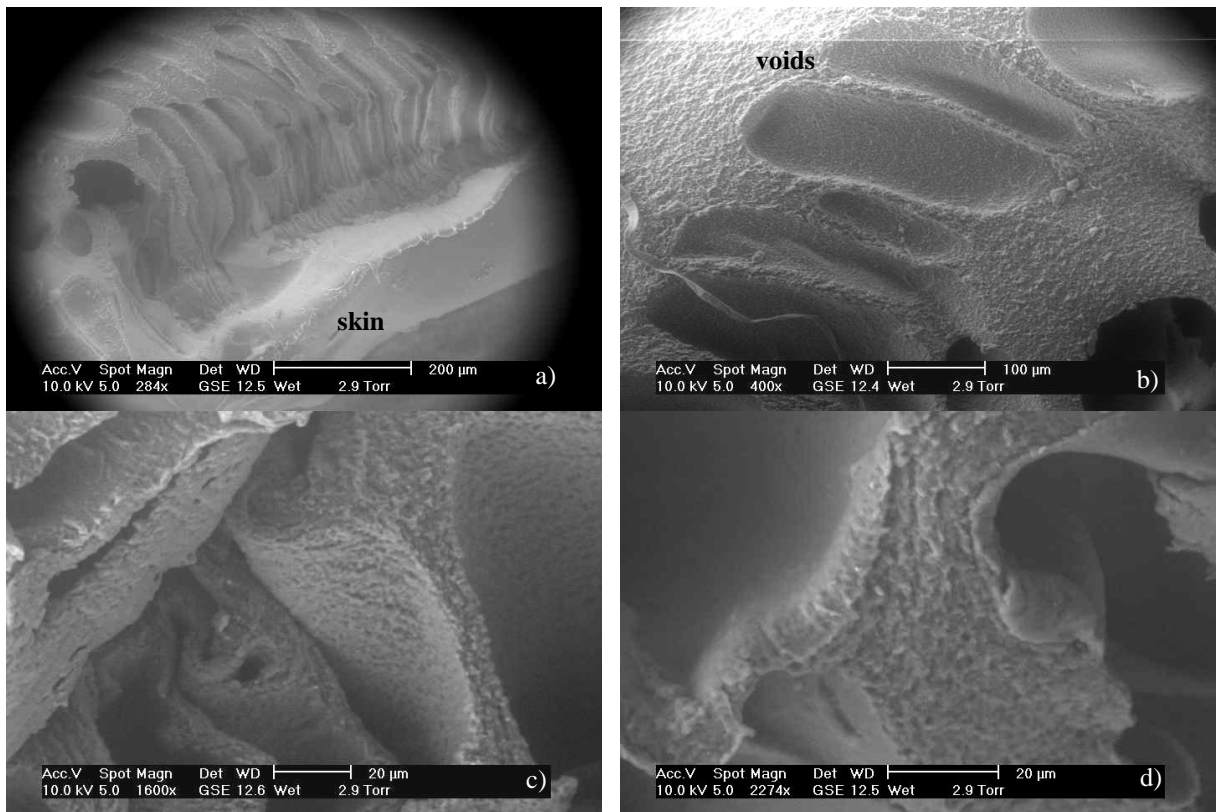


Figure 5

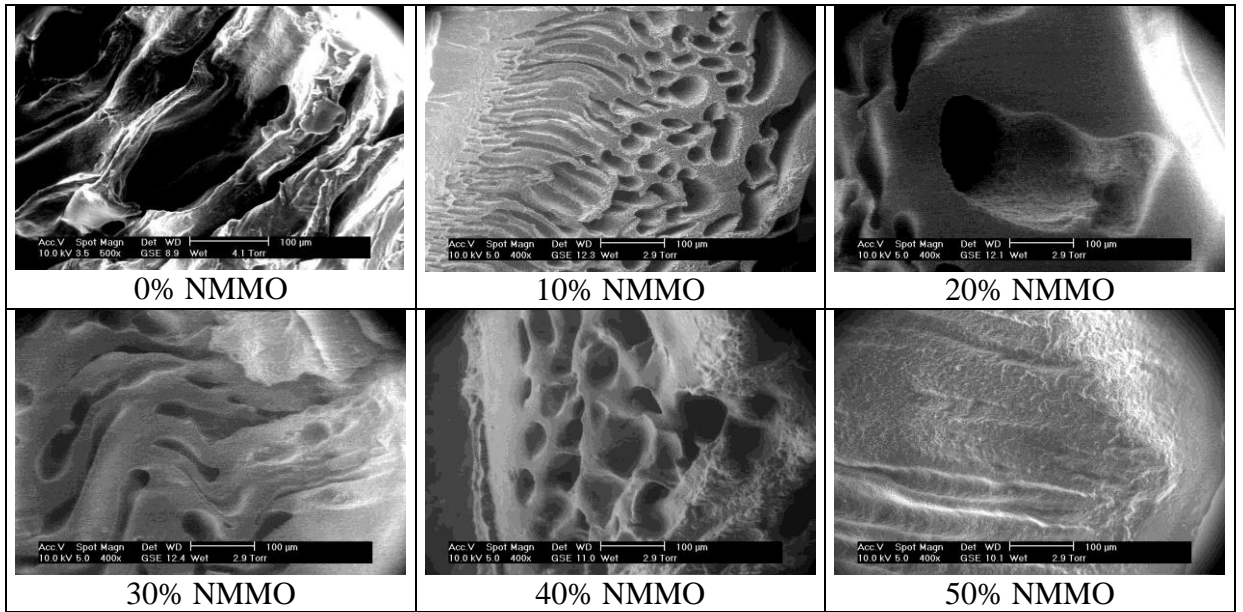
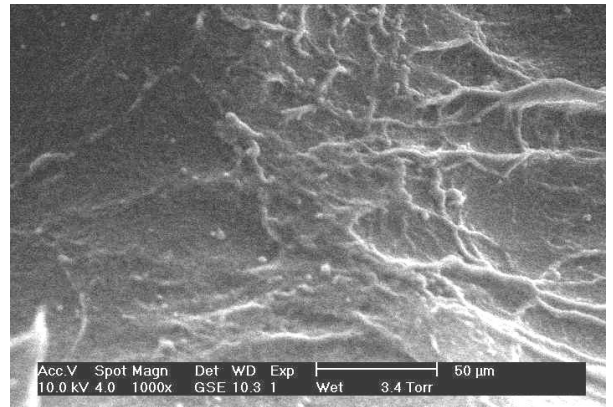
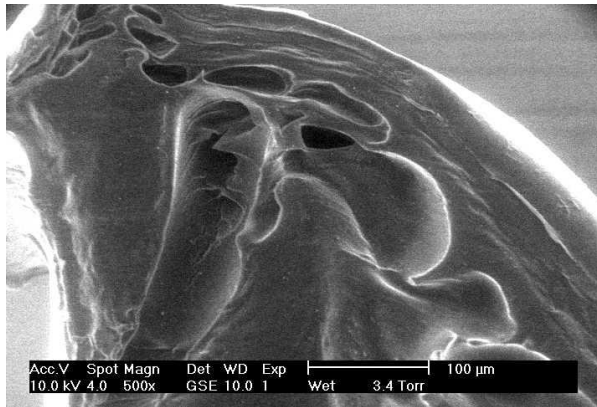
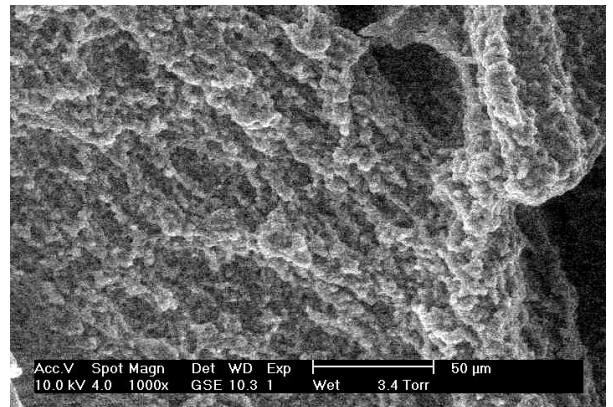
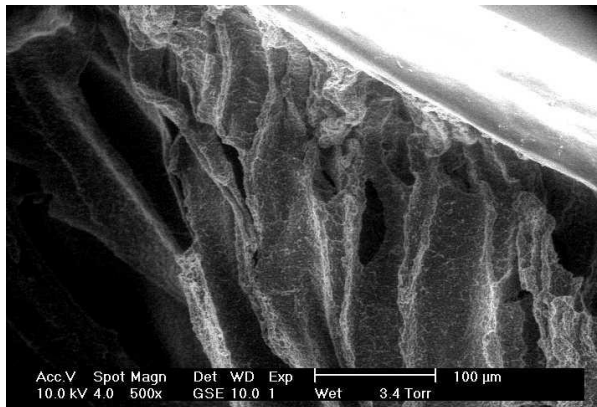


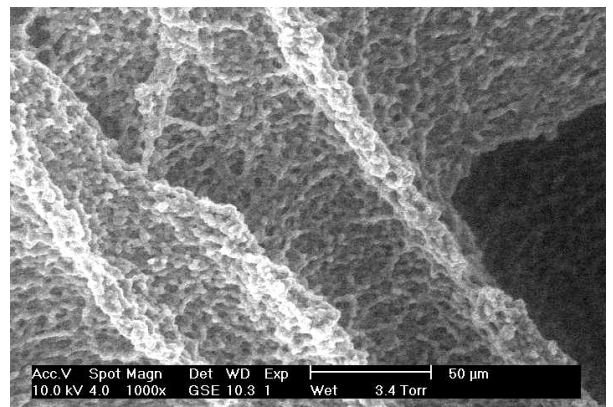
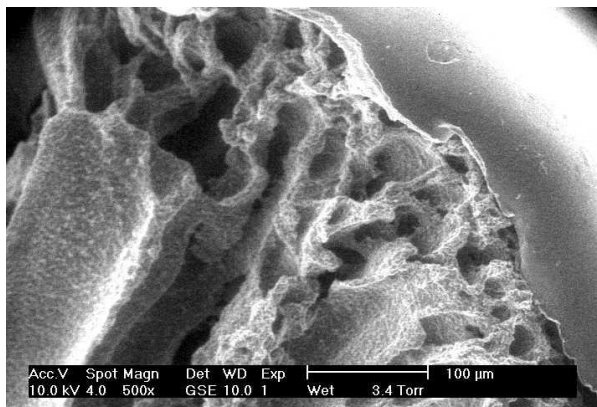
Figure 6



20°C



50°C



80°C

Figure 7

